

Flow in a Converging Channel at Moderate Reynolds Numbers

David F. James

Dept. of Mechanical Engineering, University of Toronto, Toronto, Ontario, Canada M5S 1A4

An analytical solution is found for flow in a converging channel for Reynolds numbers in the range of 10^2 to 10^3 . The solution applies to an axisymmetric channel, for which the shape is given by $R^2z = \text{constant}$, where R is the channel radius at the axial distance z . This shape produces a center-line or core velocity that increases linearly with z , thus making the extensional rate constant. The analytical solution is a pseudosimilarity solution of the axial momentum equation, and its accuracy was gauged by comparison to other results. Comparisons of velocity and pressure distributions to experimental data and to finite-element results indicate that the analytical solution is accurate to about 5%.

Introduction

This work is part of a program to develop a rheometer to measure the elasticity of non-Newtonian fluids in extensional flow. This article, however, deals with Newtonian fluids only, the results of which serve as the foundation for work on viscoelastic liquids. In this rheometer, extensional motion is produced by pushing a fluid through an axisymmetric converging channel, and the fluid's resistance to this motion is detected by pressure drop measurements along the channel. The related fluid property is termed extensional viscosity, which is defined as the normal stress in extension divided by the rate of extension, analogous to the definition of shear viscosity. In the same way that shear viscosity should be measured in a flow where the shear rate is constant, extensional viscosity should be measured in a flow where the rate of extension is constant. Hence, the converging channel should be shaped such that the fluid within is subjected to a constant rate of extension. The initial objective of the work, then, was to determine this shape for Newtonian fluids.

A basic principle of the rheometer is that Reynolds numbers are high enough to confine shear effects to the boundary layer and there is a vorticity-free zone in the core of the flow, i.e., a zone of purely extensional motion. This idea of creating an extensional zone in an internal flow follows from our earlier work on high-Reynolds-number flow in a conical channel and the measurement of extensional stress there for a dilute polymer solution (James and Saringer, 1980). In such flows, the Reynolds number must be in the range of 10^2 to 10^3 ; the Reynolds number must be high enough to create a vorticity-free zone of

some extent in the core, but not too large to make inertial stresses completely overwhelm the non-Newtonian stresses and make them undetectable. For Reynolds numbers in this range, the boundary layer is a nonnegligible fraction of the channel radius and must be taken into account when determining the channel shape that produces a constant extensional rate in the core. The desired flow field, then, is a laminar axisymmetric internal flow, in which the core velocity increases linearly with axial distance.

Analytical Approach

In this section, boundary layer techniques are used to determine the flow field at moderate Reynolds numbers. A sketch of the problem is given in Figure 1. The velocity in the inviscid core flow, U , is prescribed to be proportional to the axial coordinate z , so that the extensional rate dU/dz is constant. The problem is to find the radius $R(z)$ such that the core flow has the prescribed form. The axial and radial velocity components, inside the boundary layer, are $u(r,z)$ and $w(r,z)$, respectively.

The governing equations for steady laminar flow with no swirl are:

$$\frac{\partial}{\partial z}(ru) + \frac{\partial}{\partial r}(rw) = 0 \quad (1)$$

$$\rho \left(u \frac{\partial u}{\partial z} + w \frac{\partial u}{\partial r} \right) = - \frac{\partial p}{\partial z} + \mu \left[\frac{\partial^2 u}{\partial r^2} + \frac{1}{r} \frac{\partial u}{\partial r} + \frac{\partial^2 u}{\partial z^2} \right] \quad (2)$$

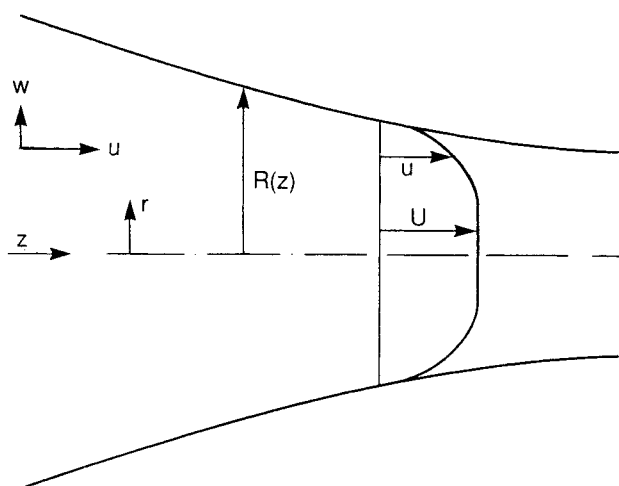


Figure 1. Flow definition in the converging channel.

$$\rho \left(u \frac{\partial w}{\partial z} + w \frac{\partial w}{\partial r} \right) = - \frac{\partial p}{\partial r} + \mu \left[\frac{\partial}{\partial r} \left(\frac{1}{r} \frac{\partial r w}{\partial r} \right) + \frac{\partial^2 w}{\partial z^2} \right] \quad (3)$$

Ordinarily these equations would be cast directly into dimensionless form, but it is preferable not to do so in this case. There are two length scales in the present problem, as in most two-dimensional boundary layer situations: l , the distance to an arbitrary axial location and, R_o , the radius at that location, which is generally much smaller than l . The axial diffusion terms in both momentum equations are, therefore, $O(R_o/l)^2$ compared to the radial diffusion terms and may be neglected. The characteristic axial velocity is taken to be U_o , the core velocity at $z=l$, and the characteristic pressure is, therefore, ρU_o^2 . By the continuity equation (Eq. 1), the corresponding characteristic radial velocity is $U_o R_o/l$. When these scalings are inserted in Eq. 3, the inertial terms and viscous terms are $O(R_o/l)^2$ and $O(\mu/\rho U_o l)$, respectively, compared to the pressure gradient. For Reynolds numbers of order 10^2 , $\partial p/\partial r$ is small and then $\rho U_o dz/dz$ can be substituted for the axial pressure gradient in Eq. 2. Since the core velocity is given by $U(z) = U_o z/l$, Eq. 2 becomes

$$u \frac{\partial u}{\partial z} + w \frac{\partial u}{\partial r} = \frac{U_o^2}{l^2} z + \nu \left[\frac{\partial^2 u}{\partial r^2} + \frac{1}{r} \frac{\partial u}{\partial r} \right]. \quad (4)$$

A similarity-solution approach is tried by letting

$$u = \frac{U_o z}{l} f'(\eta)$$

where η has the form $(R_o^2 - r^2)/z^m$. It is found that z disappears from Eq. 4 only for $m=0$, and thus η is taken to be $1 - r^2/R_o^2$. The other velocity component is then

$$w = \frac{U_o R_o^2}{2l} \frac{1}{r} f(\eta),$$

and Eq. 4 reduces to

$$(1 - \eta) f''' - f'' + K(1 + f f'' - f'^2) = 0, \quad (5)$$

where $K \equiv U_o R_o^2/4\nu l$. At the wall, u and w are zero and so two boundary conditions are $f(0) = 0$ and $f'(0) = 0$. Far from the wall, $u = U_o z/l$ and the only sensible place to apply this boundary condition is at the center-line; hence, the third boundary condition is taken to be $f'(1) = 1$.

This ordinary differential equation (ODE) looks similar to the third-order ODEs which arise in classical boundary layer solutions. Had a true boundary-layer approach been taken, distance from the wall would have been scaled with the boundary layer thickness, which is of order $\sqrt{\nu l/U_o}$ in this flow. Hence, an alternate form for η is $U_o(R_o^2 - r^2)/\nu l$ or equivalently $K(1 - r^2/R_o^2)$. With this form for η , the resulting ODE for $f(\eta)$ looks like Eq. 5 except that the coefficient for the last three terms is 1 and not K , and the coefficient of the highest order term is $K - \eta$ and not $1 - \eta$. For this alternate case, the range of η is $0 \leq \eta < K$ and the third boundary condition is $f'(K) = 1$. This latter approach is equivalent to that actually taken but is not preferred because the parameter K appears in the range of η and thus in a boundary condition. With the original approach, η has the simpler range $0 \leq \eta < 1$.

Solutions of Eq. 5 were found numerically and velocity profiles $f'(\eta; K)$ are shown in Figure 2 for several values of K . The profiles become flatter as K increases, which is expected because K is proportional to Reynolds number Re . In fact, K is equivalent to $Re R_o/8l$, where Re is defined in this instance as $2U_o R_o/\nu$. Had only one length scale been used in this problem, the free parameter would have been Re and not K . By introducing two length scales, it is learned that the solution still depends on a single parameter and that this parameter is a combination of both flow (Re) and geometry (R_o/l). That K is the appropriate parameter for this problem can also be seen when it is interpreted as the ratio of time scales, that is, when K is written in the form

$$K = \frac{R_o^2/4\nu}{l/U_o},$$

the numerator is recognized as the time for the boundary layer to diffuse a distance R_o from the wall, and the denominator is the residence time in the core flow. If the time for viscous effects to diffuse to the center-line is long compared with the

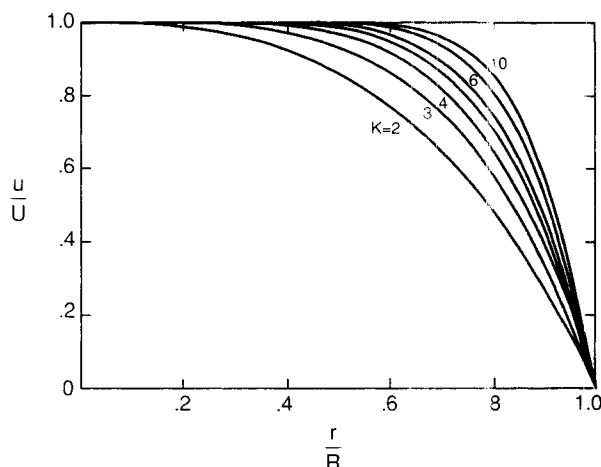


Figure 2. Velocity profiles and their dependence on K .

core residence time, then viscous effects actually extend only to a fraction of R_o , i.e., if K is large, the boundary layer is thin, as Figure 2 shows.

Our solution was developed with a converging channel in mind but it actually applies to the flow in a tube because R_o is constant. In this case, the volumetric flow rate is not constant because U increases in the flow direction; in fact, the flow rate $2\pi \int_0^{R_o} ur dr$ increases linearly with z . A closer inspection of the solution, however, reveals that the increasing flow rate is provided by a line source along the axis, i.e., the extra flow rate is provided by a discharge of magnitude $\lim_{r \rightarrow 0} 2\pi r w$ per unit length of axis. Interpreted in this way, the present solution is very similar to Brady and Acrivos's (1981) solution for flow in a tube with porous walls.

Now the approach is to ask if there is a converging channel shape, for which the present solution provides a good approximation. The shape would have to be such that the core velocity increases linearly and no fluid is introduced at the center-line. More explicitly, the shape $R(z)$ must be such that velocity profiles are given by $u = U_o z l^{-1} f'(1 - r^2/R^2)$ and such that the flow rate is constant. Since

$$Q = \frac{2\pi U_o z}{l} \int_0^R r f'(\eta) dr,$$

or

$$Q = \frac{\pi U_o R^2 z}{l} \int_0^1 f'(\eta) d\eta,$$

then the flow rate is constant if $R^2 z$ is constant. This shape, $R^2 z = \text{constant}$, is not unexpected, because streamlines in the constant-extensional-rate core are described by $r^2 z = \text{constant}$. Equivalently, $R^2 z = \text{constant}$ is the channel shape when the boundary layer is vanishingly thin.

It is proposed, then, to use the found solution for a channel whose shape is given by $R^2 z = \text{constant}$. Since the R that appears in the assumed solution is the constant R_o , it might be expected that the solution found is most accurate when R is nearly constant, i.e., for large values of z . At the same time, accuracy might be expected when K is large because of the boundary layer approach. The two expectations, however, are contradictory because K decreases as z increases. This relationship follows from the fact that K depends on an arbitrary reference location; several parameters in K vary with z and the net result is that K varies as z^{-1} . Because of the contradictory expectations, it is far from obvious where in the channel, or for what flow conditions, or for what values of K , the solution found is most accurate.

I have not been able to gauge the accuracy of our solution by analytical methods—a topic which will be addressed later; consequently, accuracy was determined by comparing the results to numerical solutions and to experimental data.

Experimental and Numerical Work

Experimental test section

A converging flow channel was made incorporating a section in which $R^2 z$ is constant. As shown in Figure 3, this test channel

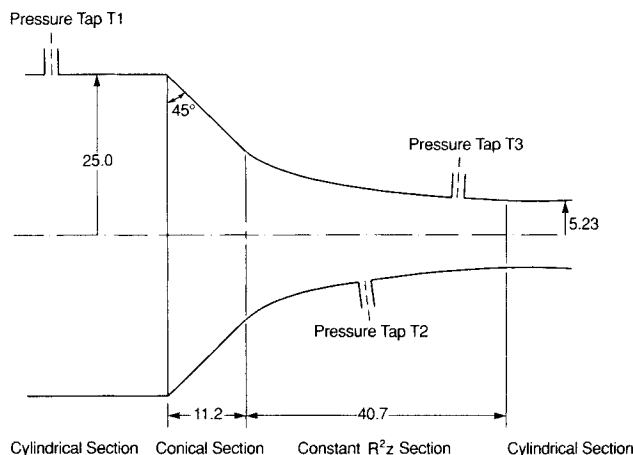


Figure 3. Scale drawing of the test channel.

All dimensions are in millimeters.

consists of an entry tube, an interjacent conical section, and the $R^2 z$ section. With a large-diameter entry tube, the initial flow is slow and its velocity profile is parabolic. The conical section is necessary to achieve high fluid strain as well as high strain rates in the $R^2 z$ section: if had the $R^2 z$ section been connected directly to the entry tube, the corner angle would have been closer to 90° than 135° and recirculation might then occur in the corner. (It would almost certainly occur with viscoelastic fluids). Distances in the $R^2 z$ section are given by $R^2 z = 1,302 \text{ mm}^3$, where the origin of z is 4.4 mm downstream of the tube-cone junction. Holes, 3.23 mm in diameter, were drilled for pressure taps: one in the entry tube 17.3 mm upstream of the junction and two in the $R^2 z$ section where the radii are 7.09 and 5.69 mm.

The test fluid was a water-glycerol mixture with a viscosity of $0.202 \text{ Pa}\cdot\text{s}$ at 25°C . This liquid was pushed through the flow cell by a custom-designed ram pump that provided constant flow rates up to $0.6 \times 10^{-3} \text{ m}^3/\text{s}$ for a minimum of 5 seconds. Pressure differences between the upstream tap and the downstream taps were measured with a calibrated pressure transducer (Celesco model P7D).

Numerical work

The dimensions of the flow cell and the properties of the fluid were supplied to Professor M. Crochet of Université Catholique de Louvain, Belgium, who used his finite-element POLY-FLOW program to compute velocities and pressures in the channel (Crochet, 1987). A parabolic profile was assumed 45 mm upstream of the tube-cone junction and the outflow was required to have vanishing normal stress and radial velocity at the end of a 7-mm tube (of radius 5.23 mm) attached to the downstream end of the channel. For flow rates of 0.25, 0.50, 1.0 and $2.0 \times 10^{-3} \text{ m}^3/\text{s}$, the program calculated the two pressure drops, the velocity profiles at the two pressure tap locations and the velocity distribution along the center-line.

The eight velocity profiles calculated by the numerical program were plotted alongside the corresponding profiles predicted by the analytical solution. Two of the eight comparisons in Figure 4 show the best and the worst agreement. The other six comparisons show that the analytical profile may be on

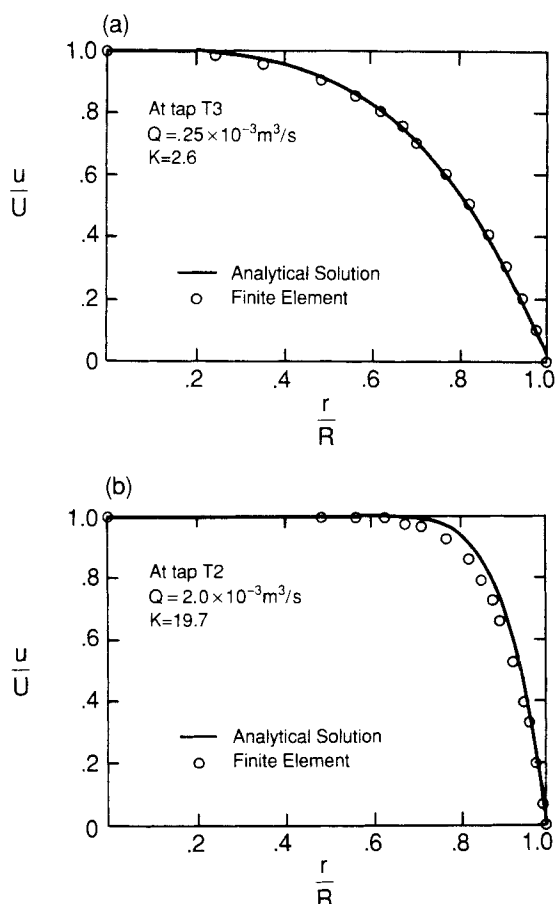


Figure 4. Velocity profiles in the R^2z section of test channel calculated by analytical solution and finite-element program.

Eight comparisons in all were made: a. best agreement and b. the worst.

either side of the numerical profile and thus agreement among the velocity profiles is good for the K range covered, which is 2 to 20. The only discernible pattern in the eight plots is that discrepancies increase as K approaches 20.

Pressure drops—analytical, numerical and experimental—were compared by plotting the pressure coefficient C_p vs. the Reynolds number Re . As usual, C_p is defined by

$$C_p = \frac{\Delta p}{\frac{1}{2} \rho V^2},$$

and the Reynolds number for these plots is taken to be

$$Re = \frac{2VR}{\nu},$$

where V and R are the mean velocity and channel radius at the relevant tap in the R^2z section. Comparisons of the two pressure drops in Figure 5 show that the analytical solution

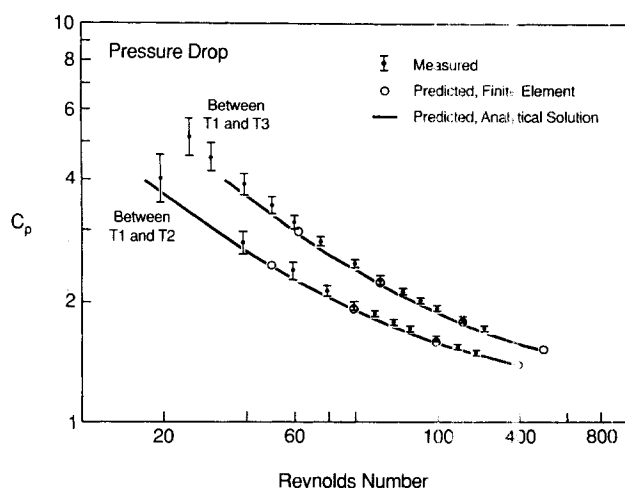


Figure 5. Pressure drops from tap 1 to tap 2 and from tap 1 to tap 3 in terms of pressure coefficient and Reynolds number.

agrees very well with the numerical predictions and both are within a few percent of the experimental data.

Figures 4 and 5 suggest that the analytical solution provides an accurate description of the flow, despite its lack of pedigree. The final quantity to check is the rate of extension in the core. This check is more demanding because the analytical solution depends on K which, as shown earlier, varies with z . Hence, the linear flow imposed on the analysis strictly applies only locally. To check overall linearity, the velocity along the center-line was computed by the finite element program for the four flow rates, and Figure 6 shows a typical result. It is apparent that the velocity does increase linearly with z over most of the

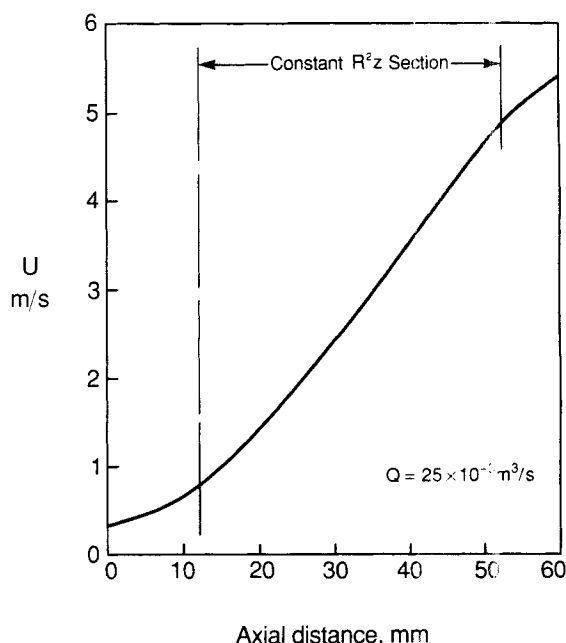


Figure 6. Velocity along the center-line of test channel as predicted by finite-element technique.

Table 1. Extensional Rates $\dot{\epsilon}$ in the R^2z Section of Test Channel

Flow Rate m^3/s	Extensional Rate $\dot{\epsilon}$	
	Analytical s^{-1}	Finite Element s^{-1}
0.25×10^{-3}	111	112
0.50	190	195
1.0	335	350
2.0	614	635

R^2z section. Values of the rate of extension $\dot{\epsilon}$ were calculated from these linear segments and compared to corresponding values from the analytical solution. There are two ways of calculating the latter value: one is to find the design value, which is just U_o/l . For a particular flow rate, U_o is found from

$$Q = 2\pi U_o \int_0^{R_o} f'(\eta) r dr$$

which yields

$$U_o = \frac{Q}{\pi R_o^2 f(1)}$$

Since $f(1)$ depends on K that depends on U_o , an iterative procedure is necessary to find U_o . This calculation is for the reference location, which was taken to be midway along the R^2z section in this case. The second way of calculating $\dot{\epsilon}$ is to find the average value over the R^2z section,

$$\dot{\epsilon} = \frac{U_2 - U_1}{z_2 - z_1},$$

where the subscripts 1 and 2 refer to conditions at the entrance and exit of the R^2z section. As might be expected, this yields a value very close to the design value and so only one (the average) is presented for comparison in Table 1. The good agreement is consistent with that shown in Figures 4 and 5.

Higher-order analyses

Because the analytical solution is demonstrably accurate and based on a similarity technique, it is natural to think that it should be the first term of an asymptotic sequence. But it is difficult to find the higher-order terms or even to suggest how they might be found.

It was argued earlier that the accuracy of this solution should be highest when dR/dz is small or when z is large. This infers an asymptotic sequence based on large z , but far downstream the boundary layer grows to fill the channel and the velocity profile becomes parabolic. This situation corresponds to $K < 1$ and implies a small K expansion. Since inertia is dominant in this problem, however, there must be a shear-free core and K is inherently $O(1)$ to $O(10)$ and far removed from small values. Hence, the solution is not a perturbation about a far downstream solution nor an expansion in small K .

Alternatively, the condition that dR/dz be small suggests an asymptotic sequence based on a perturbed boundary condition. Van Dyke (1987) recently summarized perturbation schemes and the present problem can be formulated in his terminology. His perturbation quantity ϵ is R_o/l in this situation, so that K is equivalently $Re\epsilon$. As Van Dyke notes, Manton (1971) analyzed axisymmetric tube flow for the case that $Re = O(1)$ and $\epsilon \rightarrow 0$; hence, Manton's solution pertains to nearly-parabolic profiles and $K \ll 1$, which is not relevant here. Closer to this situation is the solution developed by Williams (1963), because he based the asymptotic sequence on $Re\epsilon = O(1)$ as $\epsilon \rightarrow 0$. For slowly-varying channels, he found self-similar solutions when the radius varies exponentially with axial distance. His solution is a true similarity solution of the axisymmetric boundary layer equation, i.e., of the axial momentum equation in which the $(\partial^2 u)/(\partial z^2)$ term is omitted. This term was neglected in this case as well, but it could have been retained because the form of this solution makes this term identically zero. Hence, the present solution satisfies the full axial momentum equation and there are no neglected terms to account for in a higher-order analysis. In this problem, there are no reference lengths or velocities in the z or r direction; the only reference state is local. Consequently, it may be that each solution is valid locally, i.e., for the corresponding value of K . Therefore, the solution developed here seems to be an odd case: one that does not appear to be part of an asymptotic sequence and cannot be justified rigorously, but one which accurately describes the flow field with accuracy.

Acknowledgment

The support of the Natural Sciences and Engineering Research Council of Canada is gratefully acknowledged. Mr. Geoff Chandler made the experimental measurements.

Notation

C_p = pressure coefficient
 f = function of η
 K = dimensionless group, $U_o R_o^2 / 4\nu l$
 l = arbitrary axial location
 m = exponent of z in η
 p = pressure
 Q = volumetric flow rate
 r = radial coordinate
 R = channel radius, function of z
 R_o = channel radius at $z = l$
 Re = Reynolds number
 u = axial velocity component
 U = inviscid core velocity, function of z
 U_o = core velocity at $z = l$
 V = mean velocity, $Q/\pi R^2$
 w = radial velocity component
 z = axial coordinate

Greek letters

ϵ = small parameter, R_o/l
 $\dot{\epsilon}$ = extensional rate, dU/dz
 μ = dynamic viscosity
 ν = kinematic viscosity
 η = similarity variable, $1 - r^2/R_o^2$
 ρ = fluid density

Literature Cited

- Bird, R. B., R. C. Armstrong, and O. Hassager, *Dynamics of Polymeric Liquids*, 2nd ed., Vol. 1, Wiley, New York (1987).
- Brady, J. F., and A. Acrivos, "Steady Flow in a Channel or Tube with an Accelerating Surface Velocity—an Exact Solution to the Navier-Stokes Equations with Reverse Flow," *J. Fluid Mech.*, **112**, 127 (1981).
- Crochet, M., private communication (1987).
- James, D. F., and J. H. Saringer, "Extensional Flow of Dilute Polymer Solutions," *J. Fluid Mech.*, **97**, 655 (1980).
- Manton, M. J., "Low Reynolds Number Flow in Slowly Varying Axisymmetric Tubes," *J. Fluid Mech.*, **49**, 451 (1971).
- Van Dyke, M., "Slow Variations in Continuum Mechanics," *Adv. in Appl. Mechanics*, **25**, 1 (1987).
- Williams, III, J. C., "Viscous Compressible and Incompressible Flow in Slender Channels," *AIAA J.*, **1**, 186 (1963).

Manuscript received July 23, 1990, and revision received Nov. 20, 1990.
